Structural-Mechanical Characterization of Nanoparticle Exosomes in Human Saliva, Using Correlative AFM, FESEM, and Force Spectroscopy

Shivani Sharma,[†,‡] Haider I. Rasool,[†] Viswanathan Palanisamy,[§] Cliff Mathisen,[⊥] Michael Schmidt,[⊥] David T. Wong,[∥] and James K. Gimzewski[†,‡,¶,*]

[†]Department of Chemistry and Biochemistry, University of California, Los Angeles, California 90095, [‡]California NanoSystems Institute, University of California, Los Angeles, California 90095, [§]Department of Craniofacial Biology, MUSC College of Dental Medicine, Charleston, South Carolina 29425, [⊥]FEI Company, 5350 NE Dawson Creek Drive, Hillsboro, Oregon 97124, [∥]School of Dentistry and Dental Research Institute, University of California, Los Angeles, California 90095, and [¶]International Center for Materials Nanoarchitectonics Satellite (MANA), National Institute for Materials Science (NIMS), Tsukuba 305-0047, Japan

ABSTRACT All living systems contain naturally occurring nanoparticles with unique structural, biochemical, and mechanical characteristics. Specifically, human saliva exosomes secreted by normal cells into saliva *via* exocytosis are novel biomarkers showing tumor-antigen enrichment during oral cancer. Here we show the substructure of single human saliva exosomes, using a new ultrasensitive low force atomic force microscopy (AFM) exhibiting substructural organization unresolvable in electron microscopy. We correlate the data with field emission scanning electron microscopy (FESEM) and AFM images to interpret the nanoscale structures of exosomes under varying forces. Single exosomes reveal reversible mechanical deformation displaying distinct elastic, 70−100 nm trilobed membrane with substructures carrying specific transmembrane receptors. Further, we imaged and investigated, using force spectroscopy with antiCD63 IgG functionalized AFM tips, highly specific and sensitive detection of antigenCD63, potentially useful cancer markers on individual exosomes. The quantitative nanoscale morphological, biomechanical, and surface biomolecular properties of single saliva exosomes are critical for the applications of exosomes for cancer diagnosis and as a model for developing new cell delivery systems.

KEYWORDS: exosomes · saliva nanoparticles · nanocharacterization · force spectroscopy · CD63 membrane receptors

Characterization of naturally occurring sub-100 nm cellular nanostructures such as vaults,[1] viruses,[2] or lipid vesicles[3] has recently gained interest due to their emerging role in drug delivery or immunotherapy. In particular, exosomes are 50−100 nm particles secreted by a range of normal mammalian cells into body fluids such as saliva,[5] blood,[6] and urine[7] *via* exocytosis.[8] Although their physiological functions are unclear, recently salivary exosomes have gained significance as biomarkers for oral cancer.[4] Exosomes possess a cell-type-specific lipid-bilayer membrane containing cytosolic proteins, formed by exocytosis through an inward budding of the cell membrane.[9] Their role in specialized functions such as antigen presentation, intercellular communication, shuttling m-RNA/mi-RNA,[6,10] or infectious agents reflects a well-developed structure and functional organization of these nanovesicles.[11] Investigating individual exosomes also has important implications in understanding their fundamental physiological role and biomarker functions and for therapeutic encapsulation.[12]

Exosome characterization typically includes morphological analysis[13] which, given their nanoscale size, has been exclusively visualized with transmission electron microscopy (TEM) using stained samples precluding the possibility to obtain additional biochemical and mechanical information. Exosomes vary widely in cell-type-specific proteins and physiological conditions of the originating cell.[14] Semi-quantitative proteomic[14] and transcriptional analysis based on exosome populations[15] rather than single vesicles are inadequate for analysis of proteins/receptors on single exosomes, thus structural and surface molecular characterization on exosomes is generally lacking.

In this article, we report the substructure of human saliva exosomes based on new ultrasensitive low force AFM and correlate their nanoscale structure obtained *via* AFM with high resolution (~1 nm) low voltage, chromatic aberration corrected FESEM images. We find that the mechanical deformation of single exosomes under varying applied forces reveals a unique insight into their substructure. We detect cell-type-specific markers such as CD63 on individual

*Address correspondence to gim@chem.ucla.edu.

Received for review December 14, 2009 and accepted March 03, 2010.

Published online March 10, 2010.
10.1021/nn901824n

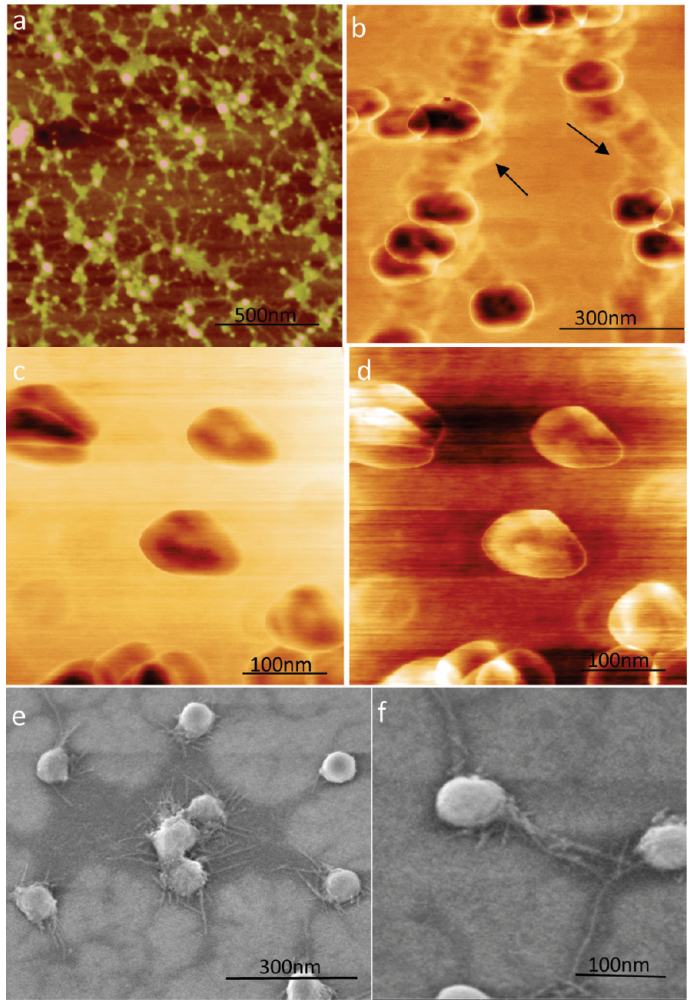

Figure 1. Ultrastructure of individual saliva exosomes observed under tapping mode AM-AFM and FESEM. (a) Tapping mode topographic AFM image showing round morphology of isolated exosomes. (b) AM-AFM phase image of aggregated exosomes. Interconnections (arrows) lacking characteristic phase shift, probably indicate some extravesicular protein content. (c) At higher forces under AM-AFM (~2 nN), representative single exosome phase images reveal trilobed substructure within the center of the vesicles. The contrast in images may be presumably attributed to variable constitutive elements (lipid, protein, RNA ratio) making up these structures. (d) Corresponding height images show a central depression of the vesicles. (e) FESEM exosome image showing multiple exosomes and (f) single isolated vesicles as round bulging structures without a central depression and well-resolved intervesicular connections.

exosomes *via* antiCD63 IgG functionalized AFM tips using force spectroscopy as well as antibody−gold beads.

RESULTS AND DISCUSSION

Structure of Human Saliva Exosomes at the Nanoscale Level. Previously, TEM imaging of numerous exosomes has revealed round vesicles with no substructure details.[15] Here AFM has enabled critical structural data comparison with parallel imaging using high-resolution FESEM while allowing additional details on physio-chemical properties of exosomes. We measured the three-dimensional structure and subvesicular organization of isolated exosomes using tapping mode AM-AFM (amplitude modulated) and PM-AFM (phase modulated) imaging, differing in the imaging force range and the feedback parameter used to generate images. Tapping mode (<1 nN force) height images of exosomes show fairly homogeneous round 50−70 nm vesicles surrounded by a network of extravesicular channels (Figure 1a). Interestingly, at larger forces (~2 nN), AM-AFM phase images reveal similar vesicle morphology (Figure 1b) with diameters of 100 ± 10 nm and indent of the vesicles in the center indicative of mechanical deformation. Channel-like elongations between exosomes appear without a prominent phase contrast, while exosomes show some aggregation without intervesicular fusion. At ~2 nN forces, single exosomes (Figure 1c) display a characteristic ring-like trilobed structure with one center appearing as a depression with characteristic phase contrast suggesting the role of heterogeneous density and/or viscoelastic image contrast mechanisms. Corresponding height images (Figure 1d) reveal overall consistent flat ~100 nm vesicles. The observed AFM phase contrast of exosomes indicates nonhomogenous surface, which is tentatively attributable to the presence of proteins and/or mRNA enclosed inside the highly dense lipid membrane, consistent with previous proteomic and RNA analysis of saliva and other exosome populations.[16] These images of single isolated sub-100 nm saliva exosome vesicles elucidate the substructural organization of exosomes unreported to date.

High-resolution FESEM exosome images show some aggregation (Figure 1e), and single isolated vesicles show round bulging structures without a central depression (Figure 1f). The images correlate well with the exosome structures obtained from AFM imaging where low imaging forces result in round, spherical shaped exosomes (Figure 1a). The extravesicular channels are well-resolved and connect the exosomes as extensions (Figure 1f). The higher magnification and lower voltage images show a very spherical surface (Figure 1f), suggesting these particles have a round morphology unless an outside force is exerted on them (*i.e.*, AFM probe). The different exosome morphologies from trilobed structures with a depression to round bulging vesicles with intervesicular connections reflect how topographical and biomechanical properties of exosomes can be explored by varying imaging feedback parameters such as force and phase set point.

Biomechanical Properties of Exosomes under Variable Forces. Biomechanical properties of vesicles[17−19] may play an important role in exocytosis and intercellular transport. We applied PM-AFM as a force nanomanipulation technique to study exosome mechanics, local deformation, and rupture characteristics. AFM image contrast exhibit combined local forces and micromechanical properties of the sample. The apparent exosome morphology changes under increasing loading force, where the force was gradually increased and then reduced, to test for elastic vesicle shape recovery. Under the high-

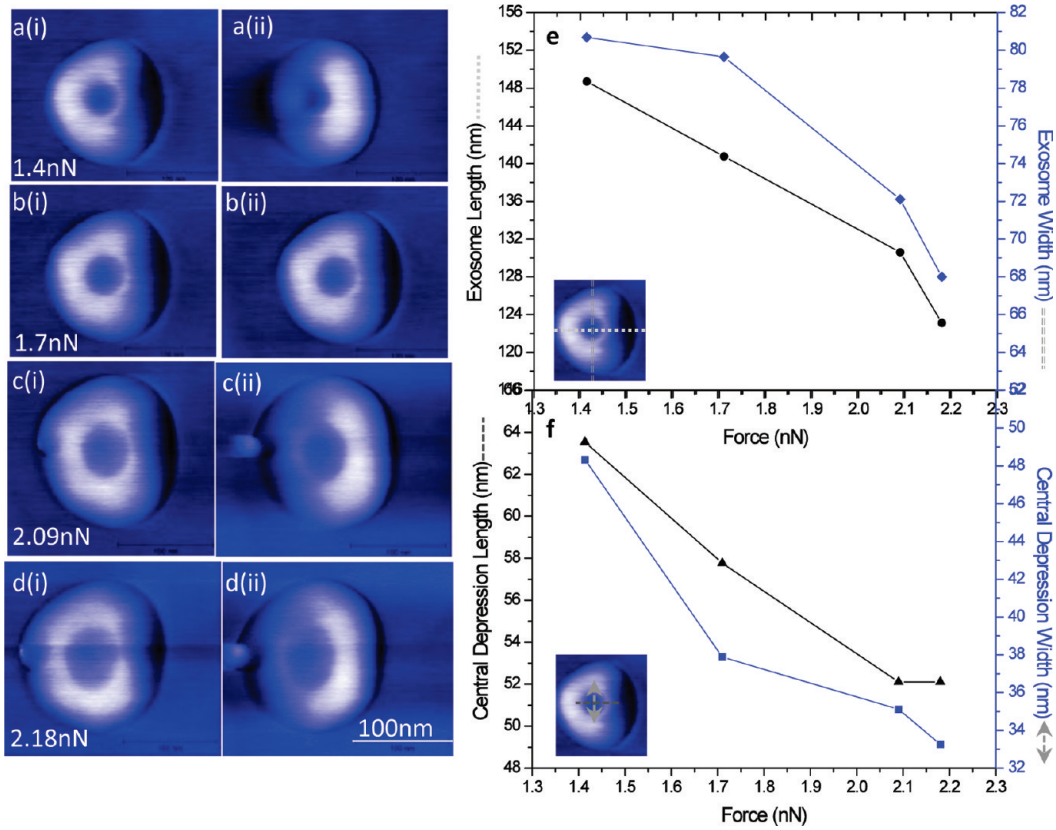

Figure 2. Mechanical deformation of single exosomes during increased imaging force under PM-AFM. (a-d) Consecutive phase images of the same exosome showing vesicle size as a function of applied force imaged under forward (i) and backward (ii) scan direction for each force set point. Increasing imaging forces (a−d) cause the overall lateral dimensions to increase and the central depression occupies more of the apparent structure. Blebbing of exosomes at high forces (c,d) a bleb or pinch observed on the exosome surfaces suggests structural perturbation. Forward tip movement possibly results in backward folding of the bleb on the exosome structure, whereas during backward scan the bleb is extended farther away from the exosome displayed as a protrusion. Bleb may result from a combination of mechanical stress well as inherent structural configuration of the exosomes. (e) Cross sectional analysis of exosome structure under varying forces. (f) Corresponding changes in the size of the central depression. The depth of the depression changes from 1.1 nm (at 1.41 nN) to 1.7 nm (at 2.18 nN).

est applied load of 2.18 nN, the vesicle appears to have the largest lateral dimensions with the central depression occupying the greatest area of the exosomes (Figure 2). The change in dimensions of the exosomes, central depression, and changes in apparent height are shown (Figure 2e,f). During high force imaging, we also observed blebbing of exosome (Figure 2), suggesting a force-induced structural perturbation. As the force was lowered during imaging, their overall lateral dimensions decrease and the central depression becomes less apparent (see Supporting Information Figure S1). Although the decrease in apparent lateral dimension can be attributed to changes in average tip−sample contact area, change in shape and disproportionate growth of the central depression is consistent with their mechanical deformation. Above 5 nN forces, exosomes reproducibly rupture into three major fragments through disintegration of the vesicular structure as well as small fragments~10 nm wide and 30 nm in length, providing an insight into dynamic modifications under applied stress (see Supporting Information Figure S1).

Surface-Biomolecular Characteristics of Exosomes Observed under Force Spectroscopy. Structural EM probes can identify receptors on vesicles[20] but are limited in structure−function studies. Two quantitative approaches to biochemical characterization of exosomes are AFM imaging of bound biofunctionalized gold beads and force spectroscopy with antiCD63 IgG functionalized tips for highly specific and sensitive detection of CD63 receptor cancer markers. Several EM techniques used functionalized gold beads to identify specific target molecules on the surface structures.[21] We used antiCD63 IgG functionalized gold beads for identification of exosome receptors by imaging under AFM. Visualization of labeled exosomes *via* antiCD63 and secondary antibody coated gold beads (Figure 3a) clearly indicates specific recognition of CD63 molecules. Multiple beads bound to exosomes indicate the presence of multiple CD63 molecules over a single membrane. This was verified by using nonspecific primary antibody as control showing no preference for exosome binding.

Figure 3b shows interaction forces between antibody-coated AFM tips and the exosome surface.

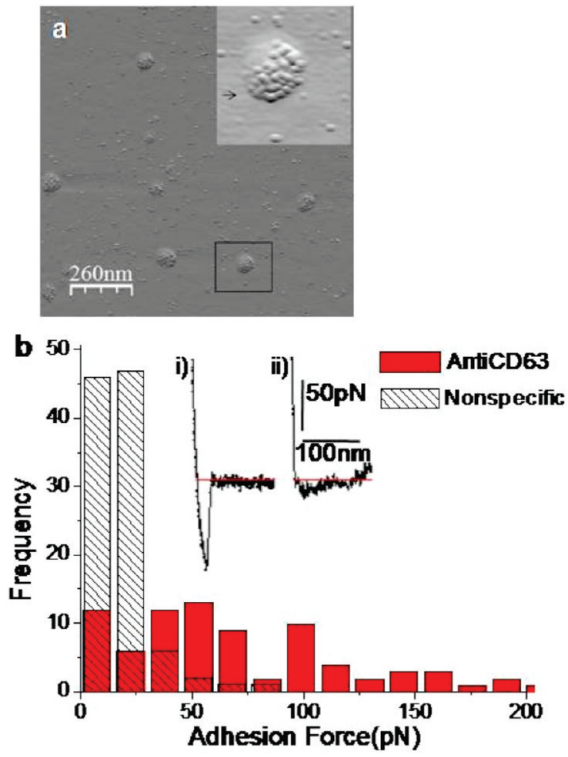

Figure 3. Biochemical characterization of exosomes *via* AFM immunogold imaging and force spectroscopy showing the presence of CD63 receptors on the exosome surface. (a) Multiple CD63 receptor sites identified with antiCD63 monoclonal antibodies and secondary antibody−gold beads. AFM topographic image showing 5−8 nm functionalized beads bound specifically to exosomes. The inset shows a zoomed out 3D image of individual beads bound to the surface of an isolated single exosome. (b) Distribution of rupture events. Nonspecific interactions occur mostly at forces <50 pN, while specific CD63 antibody-induced forces were distributed in the range of 30−200 pN. Sampled forces (n = 80 each) had each data point representing a single force measurement at any position on the exosomes surface (bin size 15 pN). Typical curves showing force (pN) as a function of separation (nm) for a single pull with (i) strong adhesive event between antiCD63 and (ii) no event for nonspecific antibody functionalized tip and exosome.

The highest rupture force was used as a measure for direct determination of the strength of the bond formed between one or multiple individual CD63 and antiCD63 pairs. Much weaker adhesive forces (<50 pN) only were observed by nonspecific antibody tips, confirming the specificity of force measurements (Figure 3b). Specific antibody tip forces were in 30−200 pN range, with the majority of the data falling between 40 and 115 pN. The mean interaction force from a normal distribution of the histogram was calculated from bins 40−115 pN as $F = 73.01 \pm 23.4$ pN (mean ± SD) and was used to estimate unbinding force between a single CD63 tetraspanin molecule and antibody. Though the exact orientation and state of antibody−antigen interaction is likely to vary, the mean interaction forces are comparable to the energy spectra of the force distribution histogram. The unbinding force is given by $F = \Delta H/d$, where ΔH is free enthalpy and d is the effective range of the potential. Typical antibody/antigen complexes with K_{ass} from 10^2 to 10^{10} M^{-1}, having free enthalpies of about 30 to 100 × 10^{-24} KJ/pair,[22] and binding pocket approximated as 0.93 nm from biotin/streptavidin data give a force of about 100pN,[23] which corresponds well with our mean force $F = 73 \pm 23$ pN (mean ± SD). Consequently, we estimate that specific adhesion peaks result from single antigen−antibody complex bond ruptures. Even higher forces (~150−200 pN) indicate the presence of multiple tetraspanin molecules constituting the vesicle surface. Presence of CD63 molecules on exosomes also suggests their endosomal instead of plasma membrane origin.[24]

CONCLUSIONS

In summary, we have demonstrated unique structural, biochemical, and mechanical characteristics of natural, biologically important human saliva exosomes at the single vesicle level. We report the distinct substructure of single isolated sub-100 nm human saliva exosomes in the form of trilobed structures and demonstrate their reversible elastic nanomechanical properties, which are constitutively secreted by normal mammalian salivary gland cells and useful as novel biomarkers for detection of pathologies such as cancer. This is demonstrated by quantitative single receptor level detection of the specific markers, CD63 receptors, on individual exosomes from human saliva *via* targeted antibody tip coated force spectroscopy and antibody-labeled gold beads. The recognition of single receptor molecules on biological fluid derived exosomes such as saliva can potentially detect pathophysiology, and thereby should enable early cancer diagnosis, where conventional methods may prove ineffective due to sensitivity limitations. Our study shows the reversible mechanical stability of exosomes under low stress while high applied forces cause structural deformation and disintegration. These data are coherent with high-resolution FESEM images. As biological nanostructures, exosomes may also provide a means to encapsulate, mimic, and enhance drug delivery systems. The characterization of naturally occurring nanostructures such as exosomes individually through size, substructure, and mechanics also provides critical data for developing engineered exosome drug delivery carriers with inherent biocompatibility and nanoarchitecture.

METHODS

Exosome Isolation and Purification: Saliva samples were obtained from healthy volunteers from the Division of Otolaryngology, Head and Neck Surgery, at the Medical Center, University of California, Los Angeles (UCLA), CA, in accordance with a protocol approved by the UCLA Institutional Review Board. All participants

gave written informed consent, and the ethics committee of UCLA approved the study. The mean age of the volunteers was 31 years (range = 26−43 years). The volunteers had no history of malignancy, immune deficiencies, autoimmune disorders, hepatitis, or HIV infection. Exosomes were prepared as described[15] with slight modifications. Briefly, 50 mL of saliva was equally mixed with phosphate buffer saline and spun at 2600*g* for 15 min to remove cells. The supernatants were then sequentially centrifuged at 12 000*g* for 20 min and 120 000*g* for 3 h. The 120 000*g* pellet was resuspended in PBS and used for AFM analysis.

AFM Imaging: Purified exosomes were diluted 1:100 in deionized water and adsorbed to freshly cleaved mica sheets, rinsed with deionized water, and dried under a gentle stream of nitrogen. The exosomes were stable without any lysis or degradation. A home-built AFM under tapping mode AM-AFM and PM-AFM and silicon probes (MPP-13220-W, spring constant, $k \sim 200$ N m^{-1}; Veeco) were used. Tapping mode AFM is based on AM-AFM, which detects the change in the vibration amplitude of the oscillating cantilever and uses it as a feedback signal to generate high-resolution images.[25] Phase images in which the phase change of the cantilever relative to the excitation signal is recorded while the feedback maintains constant vibration amplitude of the cantilever, mapping variations in material properties such as sample density and viscoelasticity. Additionally, PM-AFM enabled high-resolution images of exosomes. PM-AFM detects phase change of the oscillating silicon cantilever relative to the excitation signal and uses it as the feedback signal to obtain topographic images. Although previous studies demonstrated PM-AFM for high-resolution imaging,[26] it has not been extensively used for imaging soft biological samples. Topographic height and phase images were recorded simultaneously at 512 × 512 pixels at a scan rate of 1 Hz. Image processing was performed using Gwyddion or SPIP software.

Force Spectroscopy: For exosome immobilization, exosomes were diluted 1:50 times in PBS buffer containing 10 mM $MgCl_2$/5 mM $CaCl_2$ (pH 7.4) and adsorbed to mica surface overnight at 4 °C for stable immobilization. Samples were rinsed and imaged (Bioscope II; Veeco) under PBS in tapping mode using soft cantilevers (MSCT; Veeco) at 0.25 Hz. No significant changes were observed in the shape and size of exosomes under these conditions (see Supporting Information Figure S2). For tip functionalization, antiCD63 antibodies were attached to gold-coated AFM probes (MSCT; Veeco) *via* thiol ester linkage as described previously[27] with experimentally determined $k = 0.02$ N m^{-1}. The probes were washed in PBS, blocked with 1% BSA-PBS for 1 h, followed by rinsing with PBS. All measurements were recorded in physiological buffer conditions. Exosomes were electrostatically immobilized over mica, and AFM tip was positioned on top of the exosomes. Force−separation curves were recorded at a ramp size of 1 μm and tip velocity of 1 μm/s under low forces (<500 pN). Nanoscope software was used for data analysis. No antibody or a nonspecific mouse antibody (Anti HUR, Santa Cruz Biotechnology) coated AFM tips were used as control.

Immuno-Bead AFM Imaging: Exosomes prepared as above were incubated with 1:100 dilution of antiCD63 antibody (Santa Cruz Biotechnology, Santa Cruz, CA), followed by 20 min incubation with 1:1000 dilution secondary antibody (Molecular Probes, Invitrogen, CA) coated 10 nm gold particles (Sigma Aldrich) with consecutive PBS washes after each binding step. Samples were rinsed with deionized water, dried, and imaged under tapping mode (Bioscope II; Veeco) with silicon probes ($f = 305$ kHz, OTESPA, Veeco). Absence or nonspecific primary antibody served as controls.

Electron Microscopy: Isolated exosomes were immobilized over UV-cleaned silicon wafers. Samples were coated with iridium for 15 s at a current of 20 mA, and the wafer edges were grounded using silver paint. Vesicles were examined under low beam energies (1.5 kV at 3.1 pA) with a Magellan 400 L Extreme high-resolution FESEM (FEI Co., Hillsboro, OR).

Acknowledgment. This work was supported by WPI Center for Materials NanoArchitectonics (MANA), NIMS, Japan (J.K.G.), and National Institutes of Health Grants RO1 DE017170, UO1-DE016275 (D.T.W.) and R00DE018165 (V.P.). We thank W. Klug and J. Rim for helpful discussions.

Supporting Information Available: Reversible mechanical deformation and disintegration of single exosome under varying forces during PM-AFM imaging (S1), and AFM 3D topographic image of exosomes immobilized over mica surface imaged in buffer (S2). This material is available free of charge *via* the Internet at http://pubs.acs.org.

REFERENCES AND NOTES

1. Kickhoefer, V. A.; Garcia, Y.; Mikyas, Y.; Johansson, E.; Zhou, J. C.; Raval-Fernandes, S.; Minoofar, P.; Zink, J. I.; Dunn, B.; Stewart, P. L.; Rome, L. H. Engineering of Vault Nanocapsules with Enzymatic and Fluorescent Properties. *Proc. Natl. Acad. Sci. U.S.A.* **2005**, *102*, 4348–4352.
2. Yamada, T.; Ueda, M.; Seno, M.; Kondo, A.; Tanizawa, K.; Kuroda, S. Novel Tissue and Cell Type-Specific Gene/Drug Delivery System Using Surface Engineered Hepatitis B Virus Nano-Particles. *Curr. Drug Targets Infect. Disord.* **2004**, *4*, 163–167.
3. Cevc, G. Lipid Vesicles and Other Colloids as Drug Carriers on the Skin. *Adv. Drug Delivery Rev.* **2004**, *56*, 675–711.
4. Simpson, R. J.; Lim, J. W. E.; Moritz, R. L.; Mathivanan, S. Exosomes: Proteomic Insights and Diagnostic Potential. *Expert Rev. Proteomics* **2009**, *6*, 267–283.
5. Ogawa, Y.; Kanai-Azuma, M.; Akimoto, Y.; Kawakami, H.; Yanoshita, R. Exosome-like Vesicles with Dipeptidyl Peptidase IV In Human Saliva. *Biol. Pharm. Bull.* **2008**, *31*, 1059–1062.
6. Skog, J.; Wurdinger, T.; van Rijn, S.; Meijer, D. H.; Gainche, L.; Sena-Esteves, M.; Curry, W. T., Jr.; Carter, B. S.; Krichevsky, A. M.; Breakefield, X. O. Glioblastoma Microvesicles Transport RNA and Proteins That Promote Tumour Growth and Provide Diagnostic Biomarkers. *Nat. Cell Biol.* **2008**, *10*, 1470–1476.
7. Pisitkun, T, S. R.; Knepper, M. A. Identification and Proteomic Profiling of Exosomes in Human Urine. *Proc. Natl. Acad. Sci. U.S.A.* **2004**, *101*, 13368–13373.
8. Simpson, R. J.; Jensen, S. S.; Lim, J. W. Proteomic Profiling of Exosomes: Current Perspectives. *Proteomics* **2008**, *8*, 4083–4099.
9. Thery, C.; Ostrowski, M.; Segura, E. Membrane Vesicles as Conveyors of Immune Responses. *Nat. Rev. Immunol.* **2009**, *9*, 581–593.
10. Valadi, H.; Ekstrom, K.; Bossios, A.; Sjostrand, M.; Lee, J. J.; Lotvall, J. O. Exosome-Mediated Transfer of mRNAs And microRNAs is a Novel Mechanism of Genetic Exchange between Cells. *Nat. Cell Biol.* **2007**, *9*, 654–659.
11. Stoorvogel, W.; Kleijmeer, M. J.; Geuze, H. J.; Raposo, G. The Biogenesis and Functions of Exosomes. *Traffic* **2002**, *3*, 321–330.
12. Scheerlinck, J. P.; Greenwood, D. L. Virus-Sized Vaccine Delivery Systems. *Drug Discovery Today* **2008**, *13*, 882–887.
13. Hegmans, J. P.; Gerber, P. J.; Lambrecht, B. N. Exosomes. *Methods Mol. Biol.* **2008**, *484*, 97–109.
14. Thery, C.; Zitvogel, L.; Amigorena, S. Exosomes: Composition, Biogenesis and Function. *Nat. Rev. Immunol.* **2002**, *2*, 569–579.
15. Thery, C.; Amigorena, S.; Raposo, G.; Clayton, A. Isolation and Characterization of Exosomes from Cell Culture Supernatants and Biological Fluids. *Current Protocols in Cell Biology* 2006; Chapter 3, Unit 3 22.
16. Février, B.; Raposo, G. Exosomes: Endosomal-Derived Vesicles Shipping Extracellular Messages. *Curr. Opin. Cell Biol.* **2004**, *16*, 415–421.
17. Cross, S. E.; Jin, Y.-S.; Rao, J.; Gimzewski, J. K. Nanomechanical Analysis of Cells from Cancer Patients. *Nat. Nano* **2007**, *2*, 780–783.
18. Laney, D. E.; Garcia, R. A.; Parsons, S. M.; Hansma, H. G. Changes in the Elastic Properties of Cholinergic Synaptic Vesicles As Measured by Atomic Force Microscopy. *Biophys. J.* **1997**, *72*, 806–813.

19. Jin, A. J.; Prasad, K.; Smith, P. D.; Lafer, E. M.; Nossal, R. Measuring the Elasticity of Clathrin-Coated Vesicles *via* Atomic Force Microscopy. *Biophys. J.* **2006**, *90*, 3333–3344.
20. Melo, R. C.; Spencer, L. A.; Perez, S. A.; Neves, J. S.; Bafford, S. P.; Morgan, E. S.; Dvorak, A. M.; Weller, P. F. Vesicle-Mediated Secretion of Human Eosinophil Granule-Derived Major Basic Protein. *Lab. Invest.* **2009**, *89*, 769–781.
21. Panyi, G.; Bagdany, M.; Bodnar, A.; Vamosi, G.; Szentesi, G.; Jenei, A.; Matyus, L.; Varga, S.; Waldmann, T. A.; Gaspar, R.; Damjanovich, S. Colocalization and Nonrandom Distribution of Kv1.3 Kotassium Channels and CD3 Molecules in the Plasma Membrane of Human T Lymphocytes. *Proc. Natl. Acad. Sci. U.S.A.* **2003**, *100*, 2592–2597.
22. van Oss, C. *Nature of Specific Ligand-Receptor Bonds, in Particular the Antigen−Antibody Bond*; Marcel Dekker: New York, 1994; pp 581−614.
23. Moy, V. T.; Florin, E. L.; Gaub, H. E. Intermolecular Forces and Energies between Ligands and Receptors. *Science* **1994**, *266*, 257–259.
24. Cocucci, E.; Racchetti, G.; Meldolesi, J. Shedding Microvesicles: Artefacts No More. *Trends Cell. Biol.* **2009**, *19*, 43–51.
25. Paulo, A. S.; Garcia, R. Tip-Surface Forces, Amplitude, and Energy Dissipation in Amplitude-Modulation (Tapping Mode) Force Microscopy. *Phys. Rev. B* **2001**, *64*, 193411–193414.
26. Kobayashi, N.; Naitoh, Y.; Kageshima, M.; Sugawara, Y. High-Sensitivity Force Detection by Phase-Modulation Atomic Force Microscopy. *Jpn. J. Appl. Phys* **2006**, *45*, L793–L795.
27. Aizawa, H.; Gokita, Y.; Jong-Won, P.; Yoshimi, Y.; Kurosawa, S. Antibody Immobilization on Functional Monolayers Using a Quartz Crystal Microbalance. *Sens. J. IEEE* **2006**, *6*, 1052–1056.